Incomplete Fusion Reactions Induced by ^{12}C at 5.5–10 MeV/nucleon

I. Tserruya, V. Steiner, Z. Fraenkel, and P. Jacobs
Department of Nuclear Physics, The Weizmann Institute of Science, Rehovot, Israel

and

D. G. Kovar, W. Henning, M. F. Vineyard,[a] and B. G. Glagola
Argonne National Laboratory, Argonne, Illinois 60439
(Received 20 July 1987)

Evaporation residues following the interaction of ^{12}C with targets of ^{197}Au, ^{160}Gd, and ^{120}Sn were measured in the energy range of $E_{lab}=5.5-10$ MeV/nucleon. The experimental system allowed the determination of the cross sections of the complete fusion (CF) and the incomplete fusion (ICF) processes with a sensitivity to ICF processes below the percent level. The ICF processes were observed at all bombarding energies studied, down to energies slightly above the Coulomb barrier. The two processes have very different angular distributions, with the ICF peaked at a significantly larger angle than the CF.

PACS numbers: 25.70.Jj

The formation and decay of an equilibrated compound nucleus is the main reaction mechanism of heavy-ion collisions at low energies. At these energies, the projectile nucleus fuses with the target nucleus and the decay of the compound nucleus proceeds via the emission of light particles resulting in the formation of evaporation residues or the fissioning of the composite system. At higher incident energies this picture starts to become invalid, with reactions involving preequilibrium particle emission and projectile fragmentation or breakup becoming important. These processes lead to incomplete fusion or incomplete momentum transfer, which have attracted a great deal of interest in recent years.[1] The reaction is generally viewed[2-4] as a fast breakup of the projectile; only a part of the projectile fuses with the target nucleus while the remaining part continues nearly undeflected with approximately the beam velocity. In light systems the process is usually characterized and identified by the difference between the mean velocity of the evaporation residues and the c.m. velocity.[5-7] Alpha-particle–γ-ray coincidence measurements have also been used to study these reactions.[4,8] In heavier systems the process is identified by the correlation angle between the fission fragments relative to the correlation angle associated with full linear momentum transfer.[9,10]

In this Letter, we report measurements of cross sections for complete fusion (CF) and incomplete fusion (ICF) in collisions of ^{12}C ions with targets of ^{197}Au, ^{160}Gd, and ^{120}Sn in the energy range $E_{lab}=65-130$ MeV. The main purpose was to study the onset of the ICF process and its characteristic properties with the use of a simple and efficient detection system based on a low-pressure multistep avalanche counter. This detector and the choice of the systems mentioned above allowed us to identify the CF and the ICF components by their times of flight (TOF).

Beams of ^{12}C at 65–105 MeV were provided by the model 14UD Pelletron accelerator and the superconducting booster module of the Weizmann Institute.[11] Beams of ^{12}C at 100–130 MeV were provided by the ATLAS facility at Argonne National Laboratory. The targets consisted of $\simeq 10$-$\mu g/cm^2$ ^{197}Au, and enriched ^{160}Gd and ^{120}Sn isotopes evaporated on a 2–5-$\mu g/cm^2$ C backing. The targets were mounted at 90° with respect to the beam direction with the C backing facing the beam.

The experimental setup was very similar to the one described by Tserruya *et al.*[12] and Jacobs *et al.*[13] The evaporation residues were detected in an (8×10)-cm^2 multistep low-pressure counter. The detector[14] allows for efficient detection of heavy ions of masses up to 200 u and kinetic energies down to 1 MeV. It was centered at 0°, at 30 cm from the target, with a small Ta beam stopper, covering angles $\Theta < 1.2°$, located in front of the detector. Thus the counter covered the angular range $\Theta = 1.2-10°$ with a nearly 2π azimuthal efficiency. In a few cases the detector was centered at 15° in order to measure larger angles. Two solid-state counters mounted on opposite sides of the beam axis at $\pm 15°$ were used as monitors.

The detector was operated with a beam-current intensity ≤ 1 nA at 10^4-10^5 particles/s. Most of this yield, representing elastic-scattering events, was electronically suppressed by a delayed coincidence between the pulsed-beam signal and the time signal from the detector. Only particles having TOF >40 ns were recorded on magnetic tape on an event-by-event basis.

Evaporation residues formed after CF and ICF events were identified by their different TOF measured against the pulsed-beam signal. Table I shows some relevant kinematic values for ^{12}C on ^{197}Au at 90 MeV. Our experimental method exploits two main factors: (i) the asymmetry of the collision system which makes the TOF of

TABLE I. Kinematic quantities for $^{12}C+^{197}Au$ at 90 MeV. E, v, and TOF denote the average energy, velocity, and time of flight (over a flight distance of 30 cm) for elastic scattering (row 1), CF (row 2), and ICF under the assumption that one (row 3) or two α particles (row 4) do not fuse and escape in the beam direction with the beam velocity.

	TOF (ns)	v (cm/ns)	E (MeV)
Elastic scattering	7.9	3.8	90
CF	138	0.218	5.2
ICF $(-\alpha)$	203	0.148	2.3
(-2α)	397	0.075	0.60

elastic and quasielastic events very different from the TOF of the CF events (see Table I), and (ii) the observation that with ^{12}C projectiles the dominant ICF is associated with the emission of one or two α particles.[4] With the assumption that the α particles escape with approximately the beam velocity (see Table I), there exists a large difference between the TOF of the CF and the ICF events, and the TOF or velocity spectrum can be used to separate the evaporation residues corresponding to the CF and ICF processes. This is seen, for example, in Fig. 1, which shows the TOF and resulting velocity spectra for $^{12}C+^{197}Au$ at 105 MeV. The yields at lower TOF, which have an exponential shape, originate from slit-edge scattering somewhere upstream from the target. They are identical in shape and magnitude in measurements with target in and out. From the measurements with target out (which allow one to see the contributions of this tail in the region of interest), we conclude that the slit-edge scattering makes a negligible contribution to the CF and cannot be responsible for the ICF peak. This was verified in TOF measurements using a Si detector at 6°. The mass-versus-energy spectra obtained show that in the TOF region indicated by CF and ICF in Fig. 1 the yields are associated with heavy evaporation-residue-like yields. The dotted lines in Fig. 1(b) are the results of a two-Gaussian six-parameter fit to the data. It is seen that the main peak is exactly centered at the expected position, shown by the CF arrow, for complete momentum transfer. The ICF arrow indicates the average velocity of the evaporation residues under the assumption that one α particle escapes at zero degrees with the beam velocity. The Gaussian fit indicates that the lower peak is centered as a slightly higher velocity than expected in this simplistic scenario. In previous works,[1] based on TOF measurements, only the average velocity and the total yield of all evaporation residues were determined without separation between CF and ICF components. In this work the two-Gaussian fit was generally good and allowed us to extract the total yield of the CF and the ICF components as well as the centroid and width of their velocity distributions. Events consistent with two α particles escaping were also observed at the higher bombarding energies. Analysis of these events was not pursued, because of the unknown response of the detector to the very low kinetic energy of the residues involved (see Table I). The fraction of the yield not measured by the detector, because of the angular range subtended, was easily obtained by extrapolation of the angular distribution at small and large angles. When located at 0°, the detector measured 80%–85% of the CF yield of the Gd target at the different energies. However, at this location only 23%–37% of the ICF yield was measured for the different targets. This fraction was obtained from measurements at 90 MeV with the detector centered at 15° and it was assumed to be constant as a function of energy. Absolute cross sections were obtained by normalization of the fusion yield to the elastic yield in the monitors and by the assumption that the elastic scattering follows the Rutherford law.

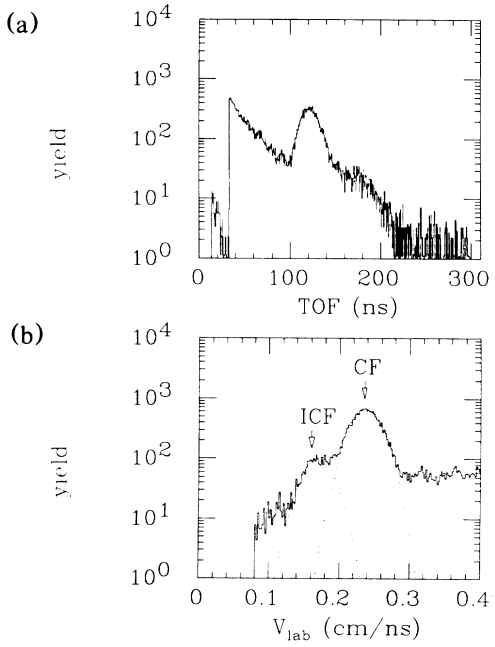

FIG. 1. (a) TOF and (b) velocity spectra for $^{12}C+^{197}Au$ at $E_{lab}=105$ MeV. The dashed lines represent a two-Gaussian fit to the CF and ICF yields. See text for meaning of the arrows.

Figure 2 shows the excitation functions extracted for the CF and the ICF processes for the ^{160}Gd target. Similar results were obtained with the other targets. The relative errors in the CF and ICF cross sections are estimated to be less than 5% and 15%, respectively. They originate primarily from the errors in the Gaussian-fit parameters and from the errors in the extrapolation of the angular distributions. The errors in the absolute cross sections due to the normalization procedure are estimated to be less than 10%. The ICF cross sections in Fig. 2 are in reasonable agreement with those reported in Ref. 4, where the same system was studied with use of the α-particle–γ-ray coincidence technique.

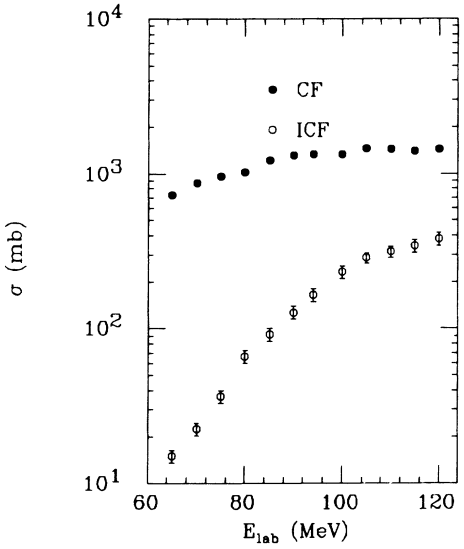

FIG. 2. Excitation functions of CF (closed circles) and ICF (open circles) for $^{12}C+^{160}Gd$.

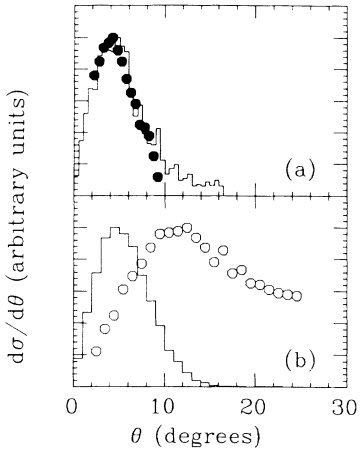

FIG. 3. Angular distribution of (a) CF and (b) ICF evaporation residues for $^{12}C+^{197}Au$ at $E_{lab}=90$ MeV. The solid lines are the results of evaporation calculations based on the code PACE for (a) $^{12}C+^{197}Au$ at 90 MeV and (b) $^{8}Be+^{197}Au$ at 60 MeV.

One sees that the magnitude of ICF increases with respect to the CF process as function of the incident energy from $\simeq 2\%$ at 65 MeV to $\simeq 27\%$ at 120 MeV. For the system $^{12}C+^{197}Au$, the ICF process represents only 0.5% of the CF component at 65 MeV. We note for reference that the Coulomb barrier of C+Au is at $\simeq 59$ MeV in the laboratory system. The ICF component was observed at all energies measured in this work. It thus appears that the ICF is present at low energies extending down to the Coulomb barrier with no apparent energy threshold for the ICF process. Recent studies[6,7,9] of linear-momentum transfer show evidence of a threshold velocity for the onset of the ICF process. When we plot, for example, the average velocity of the evaporation residues relative to the c.m. velocity as a function of the relative velocity above the Coulomb barrier (see, e.g., Refs. 1 and 7), the data for various colliding systems covering projectiles from ^{14}N to ^{20}Ne, and targets from ^{27}Al to ^{60}Ni, seem to fall on a universal curve with a common onset of ICF at $\simeq 3$ cm/ns. Our present results are not in contradiction with these studies, but rather point out their insensitivity to small ICF contributions. Our data suggest that the ICF should be viewed as a process which is always in competition with the CF process. The ICF has a low probability of $\simeq 10^{-3}$ close to the Coulomb barrier and becomes a sizable fraction of the CF cross section at about twice the Coulomb barrier.

Figures 3(a) and 3(b) show the angular distribution of $^{12}C+^{197}Au$ at 90 MeV for CF and ICF events, respectively. One essential feature should be noted from the figure. The CF angular distribution is peaked at $\simeq 4°$, while the ICF angular distribution is peaked at $\simeq 11°$ and extends to much larger angles. The CF angular distribution results only from the evaporation of light particles and it is well reproduced by calculations with the code PACE[15] [see solid line in Fig. 3(a)]. The ICF angular distribution, on the other hand, depends on the light-particle emission from the incompletely fused system and on the velocity and angular distributions of the preequilibrium or fast particles which escape fusion. The differences between Figs. 3(a) and 3(b) indicate that it is unrealistic to assume that an α particle escapes undeflected with the beam velocity. The solid line in Fig. 3(b) shows the angular distribution of the evaporation residues calculated with the code PACE under this assumption; i.e., for complete fusion of $^{8}Be+^{197}Au$ at 60 MeV. It is seen that the calculated curve is in clear disagreement with the data. In order to explain the results of Fig. 3(b) the α particle must at least have a rather broad angular distribution or be peaked at a large angle. The information obtained here is not sufficient to characterize further the mechanism of the ICF process. Coincidence measurements between the α particles and the evaporation residues would be very valuable in further clarifying this point.

To summarize, we have measured the evaporation residues following the interaction of ^{12}C with ^{197}Au, ^{160}Gd, and ^{120}Sn targets in the energy range of $E_{lab}=65-130$ MeV. The use of a low-pressure multistep counter allowed us to detect directly the evaporation residues with full efficiency down to $\simeq 1$ MeV. The choice of asymmetric systems and ^{12}C projectiles allowed for the identification of the CF and ICF events by their times of flight with a sensitivity to the ICF yield below the percent level. The ICF component was observed at all bombarding energies studied, even at energies close to the Coulomb barrier, with no apparent energy threshold. Its probability at low incident energies is very low, of the

order of 10^{-3}, and it increases steeply with bombarding energy. The angular distribution of the ICF evaporation residues is peaked at a much larger angle than those from the CF. This observation is inconsistent with the simple ICF picture in which an α particle escapes in the beam direction with the beam velocity.

One of us (I.T.) acknowledges the hospitality of Argonne National Laboratory during his stay there. This work was partially supported by the U.S.-Israel Binational Science Foundation under research grant agreement No. 84-00253.

---

[a]Present address: Department of Physics, University of Richmond, Richmond, VA 23173.

[1]See Y. Chan *et al.*, in Proceedings of the Symposium on the Many Facets of Heavy Ion Fusion Reaction, Argonne, Illinois, 1986 (to be published), for a review of incomplete fusion reactions.

[2]D. R. Zolnowski, H. Yamada, S. E. Cala, A. C. Kahler, and T. T. Sugihara, Phys. Rev. Lett. **41**, 92 (1978).

[3]T. Udagawa and T. Tamura, Phys. Lett. **116B**, 311 (1982).

[4]K. Siwek-Wilczyńska, E. H. du Marchie Van Voorthuysen, J. Van Popta, R. H. Siemssen, and J. Wilczyński, Phys. Rev. Lett. **42**, 1599 (1979), and Nucl. Phys. **A330**, 150 (1979).

[5]H. Morgenstern, W. Bohne, K. Grabish, D. G. Kovar, and H. Lehr, Phys. Rev. Lett. **113B**, 463 (1982).

[6]Y. Chan. M. Murphy, R. G. Stokstad, I. Tserruya, S. Wald, and A. Budzanowski, Phys. Rev. C **27**, 447 (1983).

[7]G. S. F. Stephans, D. G. Kovar, K. V. F. Janssens, G. Rosner, H. Ikezoe, B. Wilkins, D. Henderson, K. T. Lesko, J. J. Kolata, C. K. Gelbke, B. V. Jacak, Z. M. Koenig, D. G. Westfall, A. Szanto de Toledo, E. M. Szanto, and P. L. Gohthier, Phys. Lett. **161B**, 60 (1985).

[8]T. Inamura, M. Ishihara, T. Fukuda, T. Shimoda, and H. Hiruta, Phys. Lett. **68B**, 51 (1977).

[9]V. E. Viola, B. B. Back, K. L. Wolf, T. C. Awes, C. K. Gelbke, and H. Prever, Phys. Rev. C **26**, 178 (1982).

[10]M. B. Tsang, D. R. Klesch, C. B. Chitwood, D. J. Fields, C. K. Gelbke, W. G. Lynch, H. Utsunomiya, K. Kwiatkowski, V. E. Viola, and M. Fatyga, Phys. Lett. **134B**, 169 (1984).

[11]I. Ben-Zvi, B. V. Elkonin, J. S. Sokolowski, and I. Tserruya, Nucl. Instrum. Methods Phys. Res., Sect. A (to be published).

[12]I. Tserruya, P. Jacobs, A. Breskin, R. Chechik, Z. Fraenkel, S. Lantzman, U. Smilansky, and N. Zwang, in *Fusion Reactions Below the Coulomb Barrier,* edited by S. G. Steadman, Lecture Notes in Physics Vol. 219 (Springer-Verlag, Berlin, 1985), p. 325.

[13]P. Jacobs, Z. Fraenkel, G. Mamane, and I. Tserruya, Phys. Lett. B **175**, 271 (1986).

[14]A. Breskin, R. Chechik, Z. Fraenkel, P. Jacobs, I. Tserruya, and N. Zwang, Nucl. Instrum. Methods Phys. Res., Sect. A **221**, 363 (1984).

[15]PACE is the modification of the code JULIAN described by A. Gavron, Phys. Rev. C **21**, 230 (1980).